Article

Correlation between Peak Height of Polar Mesospheric Clouds and Mesopause Temperature

Yuxin Li [1,2], Haiyang Gao [1,2,*], Shaoyang Sun [1,2] and Xiang Li [2]

[1] Key Laboratory for Aerosol-Cloud-Precipitation of China Meteorological Administration, Nanjing University of Information Science and Technology, Nanjing 210044, China; liyuxin@nuist.edu.cn (Y.L.); sunshaoyang@nuist.edu.cn (S.S.)

[2] School of Atmospheric Physics, Nanjing University of Information Science and Technology, Nanjing 210044, China; lixiang@nuist.edu.cn

[*] Correspondence: gaohy@nuist.edu.cn

Abstract: Polar mesospheric clouds (PMCs) are ice crystal clouds formed in the mesosphere of high-latitude regions in both the northern (NH) and southern hemispheres (SH). Peak height is an important physical characteristic of PMCs. Satellite observation data from solar occultation for ice experiments (SOFIE) during seven PMC seasons from 2007 to 2014 show that the difference between the height of the mesopause and the peak height of the PMCs (Z_{mes}-Z_{max}) were inversely correlated with the atmospheric mesopause temperature. The Z_{mes}-Z_{max} averages for all seasons for the NH and SH were 3.54 km and 2.66 km, respectively. They were smaller at the starting and ending stages of each PMC season and larger in the middle stages. Analysis of the individual cases and statistical results simulated by the PMCs 0-D model also revealed the inverse correlations between the Z_{mes}-Z_{max} and mesopause temperature, with correlation coefficients of -0.71 and -0.62 for the NH and SH, respectively. The corresponding rates of change of Z_{mes}-Z_{max} with respect to mesopause temperature were found to be -0.21 km/K and -0.14 km/K, respectively. The formation mechanism of PMCs suggests that a lower temperature around the mesopause can lead to a greater distance and longer time for ice crystals to condense and grow in clouds. Thus, ice crystals sediment to a lower height, making the peak height of the PMCs further away from the mesopause. In addition, disturbances in small-scale dynamic processes tend to weaken the impact of temperature on the peak height of PMCs.

Keywords: polar mesospheric clouds; cloud peak height; mesopause; atmospheric temperature; correlation

1. Introduction

Polar mesospheric clouds (PMCs), also known as noctilucent clouds (NCLs) observed from the ground, are extremely thin (approximately 3 km-thick) ice crystal clouds that form approximately 83 km above the Earth's surface in high-latitude regions (above 50°) in both the northern (NH) and southern hemispheres (SH). During twilight periods, PMCs have the unique ability to reflect sunlight below the horizon, showcasing charming and spectacular scenery. PMCs are commonly observed in the NH from mid-May to August and in the SH from mid-November to February. These periods are commonly referred to as the PMC seasons. The frequency of PMCs and their observed brightness have increased over the past half-century [1]. In recent years, PMCs have appeared frequently in mid-latitude regions (30–50°) [2]. Previous studies have shown a strong association between these phenomena and the greenhouse effect in the lower atmosphere and long-term climate change [3–5], attracting increasing attention from the scientific community.

In addition to cloud-top and cloud-bottom heights, the peak height of PMCs is an important physical quantity used to describe their characteristics. In practical observations, the peak height of PMCs can be defined as the height at which the observed radiation,

extinction, or scattering coefficients are maximized, depending on the observation method and instrument configuration [6,7]. In modeling simulations, the peak height of PMCs is typically defined as the height at which the ice mass density or volume density is at its maximum [8]. The peak height of PMCs is typically around 83 km in the upper region of the mesosphere, but it is highly variable, with a range of up to ±3–5 km [9]. Because this altitude is similar to that of the mesopause (85–92 km) and the evolution of clouds is highly influenced by background atmospheric conditions, such as temperature and water vapor, previous studies have suggested that there may be a certain correlation between the peak height of PMCs and the height of the mesopause [10–13]. Russell et al. (2010) [11] proposed that the peak height of the PMCs during the first half of the season is consistently located approximately 3.5 km below the mesopause, with minimal differences between the NH and SH. Bailey et al. (2005) [14] analyzed satellite data prior to 2005 and found that the peak height of the PMCs was located approximately 2.5 km below the mesopause, with differences between the NH and SH reaching 1.0–1.5 km. Using ground-based lidar measurements, Chu X et al. (2004) [15] found that the peak height of PMCs was 83.74 ± 0.25 km, with a 1.3 km difference between the NH and SH. Through modeling studies, Jensen et al. (1988) [16] demonstrated that the peak height at which ice crystals of maximum size were present were approximately 3–4 km below the mesopause. Recent modeling studies using a two-dimensional aerosol and cloud radiative microphysical model (CARMA) have indicated larger differences between the altitude of the mesopause and the peak height of PMCs, with differences of 5–7 km and 3–4 km in the SH and NH, respectively [17]. However, some studies have suggested that the relationship between these two parameters remains unclear. For instance, Lübken et al. (2007) [18] analyzed PMC information obtained through falling sphere techniques and lidar measurements combined with simultaneous temperature measurements and found no significant correlation between the altitude of the mesopause and the altitude of the PMC layer. There are limitations in studying the correlation between the altitude of the mesopause and the altitude of PMCs because of the relatively low vertical spatial resolution of commonly used satellite limb observations, such as sounding of the atmosphere using broadband emission radiometry (SABER) and a microwave limb sounder (MLS) (2–4 km), as well as constraints on ground-based lidar observations, which are limited to local measurements.

During the summer season in both the NH and SH, the mesopause region is the coldest area in Earth's atmosphere, where the temperature sometimes reaches as low as 120 K. At such low temperatures, even a small amount of water vapor (mixing ratio > 0.01 ppmv) can reach supersaturation, leading to the formation of PMCs [19]. The mechanism underlying the formation of PMCs suggests that ice crystals initially form in slightly higher regions of the mesopause and then grow through condensation during descent until they reach visible sizes. The ice crystal size and mass density reach their maximum values at a certain height below the mesopause, and as the ice crystals continue to fall, the background atmospheric temperature increases, causing the rapid dissipation of clouds [8]. Previous research has shown that the water vapor content is relatively stable with a mixing ratio of 5~10 ppmv in the mesopause region during PMC formation, particularly during the beginning and ending stages of the PMC season, whereas temperature variations have a more significant impact on cloud formation and evolution [19]. Based on condensation and sublimation mechanisms, it is inferred that there is a correlation between the peak height of PMCs and the altitude of the mesopause. However, the difference between them is influenced by the mesopause temperature, and the values are not constant but rather exhibit certain patterns of variation. This study sought to validate this inference using satellite data with higher vertical resolution and a PMC model.

2. Data and Models

2.1. SOFIE/AIM Data

The Aeronomy of Ice in the Mesosphere (AIM) satellite, developed by NASA, was launched on 25 April 2007. This was the first satellite specifically designed to study PMCs.

AIM carries three payloads, one of which is the Solar Occultation For Ice Experiment (SOFIE). SOFIE uses measurements of the extinction characteristics at 16 wavelengths ranging from 0.29 to 5.32 μm to retrieve parameters related to PMCs in the altitude range from 20 to 95 km. In this work, the parameters from level 2 data, including vertical profiles of temperature, water vapor, mesopause altitude, PMC peak, top, bottom heights, and ice mass density, were used. Owing to its polar orbit and occultation observation mode, SOFIE can only conduct effective observations at 15 sunrise and 15 sunset moments each day. Therefore, every observation corresponds to only one specific latitude. The latitude is shown in Figure 1. However, it has high precision and sensitivity, especially with a vertical spatial resolution of 0.2 km, which is well suited to the objectives of this study [20]. SOFIE carried out stable observations from 2007 to 2015, covering latitudes between 60° and 85° during the PMC seasons in both the NH and SH. From 2016 to 2018, the coverage area shifted to the mid-latitudes because of orbital changes. The data quality of the PMC observations decreased after the orbit was restored in 2019, and the AIM satellite mission concluded in March 2023. Therefore, this study used level 2 data from seven PMC seasons in each hemisphere from 2007 to 2014. A complete PMC season typically lasts 70–100 d and is conventionally recorded using the summer solstice in each hemisphere as a reference point.
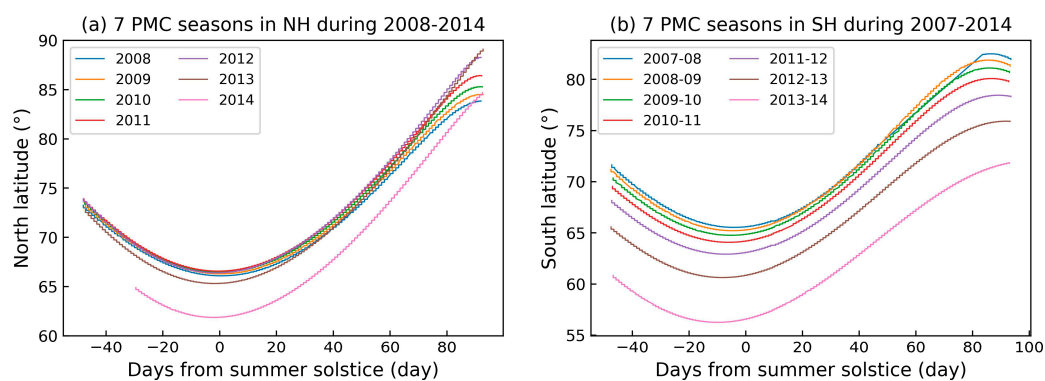
Figure 1. Latitude of SOFIE observation data for 7 PMC seasons in the NH (**a**) and SH (**b**), respectively, from 2007 to 2014.

2.2. 0-D PMC Model

Hervig et al. (2009) [21] developed a zero-dimensional (0-D) model for PMCs (referred to hereinafter as the 0-D model) based on the thermodynamic equilibrium of ice particles. This model is used to simulate the relationship between the ice mass density and altitude of PMCs. This model does not consider microphysical processes extensively and ignores the time dependence of ice crystal growth, sedimentation, horizontal and vertical transport, and sublimation. The results of the 0-D model are closer to the critical state of complex microphysical models, such as CARMA [17]. The model has two options for calculating supersaturation: MK03 [22] and MK05 [23]. The MK05 scheme was chosen in this study because it yields higher accuracy than MK03 in simulating the vertical structure of cloud layers.

3. Analysis of Observational Results

3.1. Distribution of Peak Height of PMCs and Mesopause Altitude

We analyzed level 2 data from seven PMC seasons in each hemisphere obtained by SOFIE from 2007 to 2014. The temperature profiles are represented by rainbow-colored contour backgrounds in Figure 2.
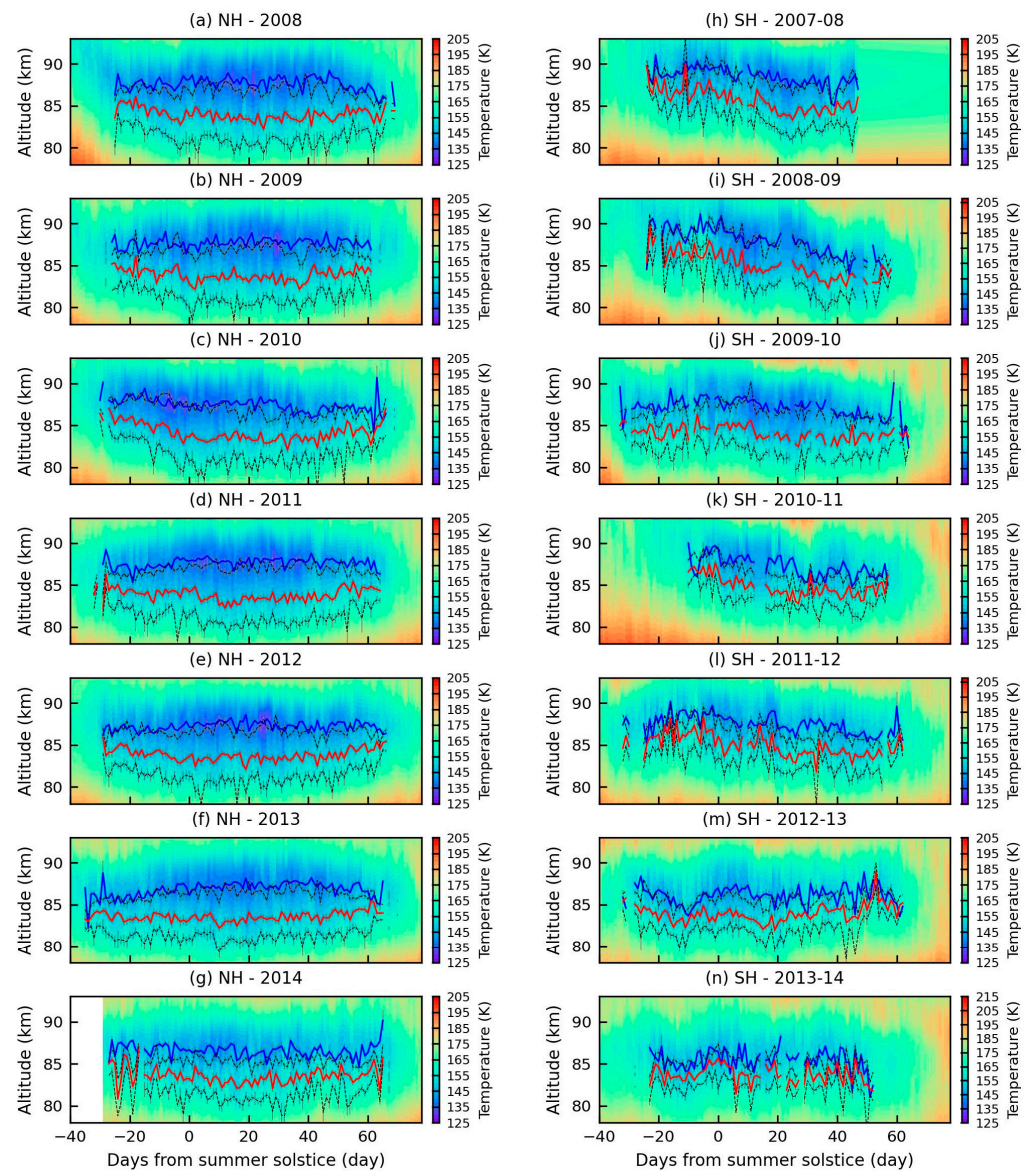
Figure 2. The distributions of daily temperature profile (rainbow background), mesopause height (blue curves), peak height of PMCs (red curves), and cloud top and cloud bottom (black curves) observed by SOFIE for 7 PMC seasons in the NH (**a**–**g**) and SH (**h**–**n**) from 2007 to 2014, respectively. Error bars show the standard deviation of the daily mean (Grey vertical line). Note that the blank area in panel (**g**) indicates no observation data from SOFIE during those days.

The mesopause altitude (Z_{mes}) was defined as the height at which the lowest temperature was observed within a range of 70 to 100 km. For identification of ice layers, it was noted that the profiles of band 9 (3.064 µm) were used because its extinction was greater than twice the noise (i.e., 10^{-7} km^{-1}) [24]. Thus, the threshold for ice detection was effectively when the extinction of band 9 (3.064 µm) was greater than 2×10^{-7} km^{-1}. The cloud top (Z_{top}) was defined as the first occurrence of the threshold from top to bottom, while the cloud bottom (Z_{bot}) was that from bottom to top. The peak height (Z_{max}) of the PMCs was defined as the height at which the mass density profile of clouds reached its maximum value. We calculated the daily mean and the standard deviation of the daily mean from 15 observations conducted each day. The results are shown as the blue and red curves in Figure 2. The results obtained for the NH indicate that the duration of a complete PMC season was typically 90–100 d, which corresponds to approximately 30 d before and 70 d after the summer solstice. The mesopause altitude was typically distributed within

a range of 86–90 km; however, its variation over time within the season was inconsistent. The peak height of the PMCs was generally located below the mesopause altitude and typically ranged from 82 to 86 km. The difference between the two altitudes showed a similar trend over time, with smaller values at the beginning and end of the season and larger values in the mid-season. These findings differ from the constant difference of 3.5 km mentioned in reference [11]. The white curve in Figure 2 also indicates the proximity between the cloud-top altitude and mesopause altitude. This was determined by the mechanism through which cloud formation initially occurred in the coldest regions of the background atmosphere.

The distribution patterns in the SH and NH exhibited some differences. Except for the incomplete data for the 2007–2008 season, the time spans of the PMC seasons varied significantly. For example, the 2010–2011 season lasted only 67 days, whereas the 2009–2010 season lasted 94 days. The mesopause temperature in the SH was slightly higher during the PMC season than in the NH, especially at the beginning and end of the season. The temperature often remained near the critical value of the frost point temperature. When the water vapor difference is small, temperature fluctuations and changes caused by dynamic processes in the middle layer are more likely to trigger the formation or dissipation of PMCs [19]. Consequently, the time spans of the PMC seasons varied greatly by year. Furthermore, the mesopause altitude varied significantly over time in the SH, which, in turn, led to fewer apparent variations in the peak height of PMCs directly below it compared to the NH. Additionally, the difference between the mesopause altitude and the peak height of PMCs was smaller in the SH than in the NH.

Previous studies have shown that some characteristics of PMC, such as occurrence frequency, ice water content (IWC), PMC layer height, microphysical features, etc., are latitude dependent, mainly because the temperature and water vapor that control the formation of noctilucent clouds exhibit significant changes in latitude. Even the long-term variation trend of PMCs also has latitude differences, which are more pronounced at high latitudes. Generally, when studying the distribution of PMC in time and latitude using satellite data, limb observation mode satellites are commonly used. This observation method can cover a wide latitude range at different time periods, if the inclination of the satellite orbit is appropriate. But the problem with such instruments is the lower vertical spatial resolution due to the inversion algorithm of onion peeling. In contrast, the occultation observation mode has a high vertical spatial resolution but can only obtain high-quality data at sunrise and sunset every orbit period, resulting in very limited latitude coverage. Daily observations can only correspond to one latitude, such as SOFIE. This makes it impossible for us to study the distribution characteristics of PMC at different latitudes within a period. This is also a part that is lacking in this study. Fortunately, it is possible that in the future, we will be able to use spaceborne active remote sensing instrument such as LiDAR to observe PMCs with extremely high spatiotemporal resolution. The spaceborne LiDAR carried by EARTHCARE, which is already in orbit, will have great potential for our application [25,26].

3.2. The Correlation between the Peak Height of PMCs and the Mesopause Temperature

To analyze the relationship between the peak height of PMCs and the mesopause temperature, we considered two PMC seasons: the 2012 season in the NH and the 2012–2013 season in the SH. As Figure 3a shows, the NH season started 31 d before the summer solstice (21 May 2012) and ended 66 d after the summer solstice (24 August 2012). The red curve represents the peak height of the PMCs, which is the height at which the ice mass density profile reaches its maximum value. Over time, this curve initially increased, then decreased, and then increased again. The average value for the entire season was 83.82 km. The yellow curve represents the mesopause altitude, which exhibited the opposite trend. The average mesopause altitude was 87.21 km. In this study, we focused on the difference between the mesopause altitude and the peak height of the PMCs (Z_{mes}-Z_{max}). The difference is shown in Figure 2b. Over time, Z_{mes}-Z_{max} exhibited a distribution pattern

with smaller values (approximately 2 km) at the starting and ending stages and larger values (approximately 5 km) in the middle of the PMC season. The average value for the entire season was 3.39 km. Figure 3c illustrates the variation in mesopause temperature, which exhibited a clear inverse trend with the peak height of the PMCs. It tended to be higher at the start and end of the season and lower during the middle period. The average mesopause temperature for the entire season was 138.05 K.
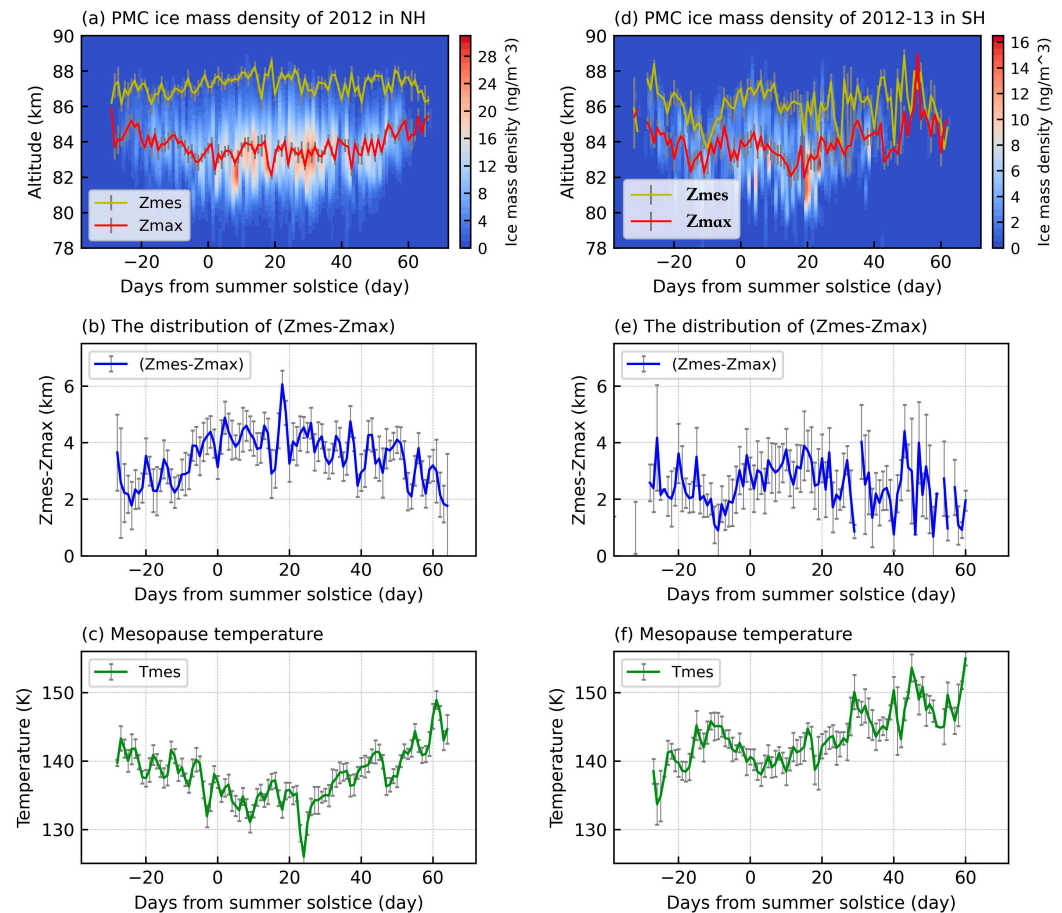

Figure 3. The distributions of daily mean ice mass density, Z_{mes}-Z_{max}, and mesopause temperature in the NH season of 2012 (**a**–**c**) and the SH season of 2012~2013 (**d**–**f**). Error bars show the standard deviation of the daily mean (grey vertical line).

Compared to that in the NH, the PMC season in the SH during 2012–2013 was relatively complex. As Figure 3d shows, the season lasted 97 days, starting 33 days before the summer solstice (18 November 2012) and ending 63 days afterward (23 February 2013). The peak height of PMCs did not exhibit a stable trend over time, and the average value for the entire season was slightly higher than for the NH, at 84.00 km. Unlike that in the NH, the mesopause altitude in the SH did not exhibit an inverse trend with the peak height of PMCs. Instead, it displayed a similar variation trend, with an average value of 86.11 km, approximately 1.1 km lower than for the NH, which is consistent with the findings of previous studies [27]. Figure 3e shows that the variation in Z_{mes}-Z_{max} over time in the SH was not stable, with an average value of 2.31 km, smaller than that for the NH by 1.08 km. However, as Figure 3f shows, the temperature variation at the mesopause altitude exhibited a clear inverse correlation with Z_{mes}-Z_{max}. The average mesopause temperature for the entire season was 143.64 K, which was 5.59 km higher than that for the NH. The higher temperature is not conducive to the formation and condensation growth of ice crystals in PMCs. It also leads to the early dissipation of ice crystals at higher altitudes during their descent. This is the main reason why Z_{mes}-Z_{max} was smaller in the SH than in the NH.

Additionally, it is also the primary reason for the lower ice mass density of PMCs in the SH shown in Figure 3d compared to that shown for the NH in Figure 3a.

As Figure 3 shows, there was a clear inverse trend between Z_{mes}-Z_{max} and the mesopause temperature. We conducted a statistical analysis of the correlation using data from seven PMC seasons each from the NH and SH from 2008 to 2014. The results are shown in Figure 4. Data for a total of 624 days of valid data for the seven seasons of the NH were analyzed. As Figure 4a shows, the correlation coefficient between Z_{mes}-Z_{max} and the mesopause temperature of the middle layer was -0.59. By linear regression, we obtained the equation Z_{mes}-$Z_{max} = -0.14T_{mes} + 23.08$, indicating that Z_{mes}-Z_{max} changed at a rate of -0.14 km/K regarding the mesopause temperature T_{mes}. The average mesopause temperature for the seven seasons was 138.16 K, and the average value of Z_{mes}-Z_{max} was 3.54 km. In comparison, the correlation shown in Figure 4b for the PMC seasons in the SH was slightly weaker. There were 408 days of valid data for the seven seasons. The correlation coefficient between Z_{mes}-Z_{max} and the mesopause temperature was -0.37. We linearly fitted the data and obtained the equation Z_{mes}-$Z_{max} = -0.08T_{mes} + 14.52$. In contrast to that in the NH, Z_{mes}-Z_{max} in the SH changed at a smaller rate of -0.08 km/K regarding the mesopause temperature T_{mes}. The average mesopause temperature for the seven seasons was higher, at 142.01 K, and the corresponding average value of Z_{mes}-Z_{max} decreased to 2.66 km. This difference indicates that the influence of temperature on Z_{mes}-Z_{max} was more pronounced in the NH, suggesting that the effect of temperature is more significant under colder background atmospheric conditions.
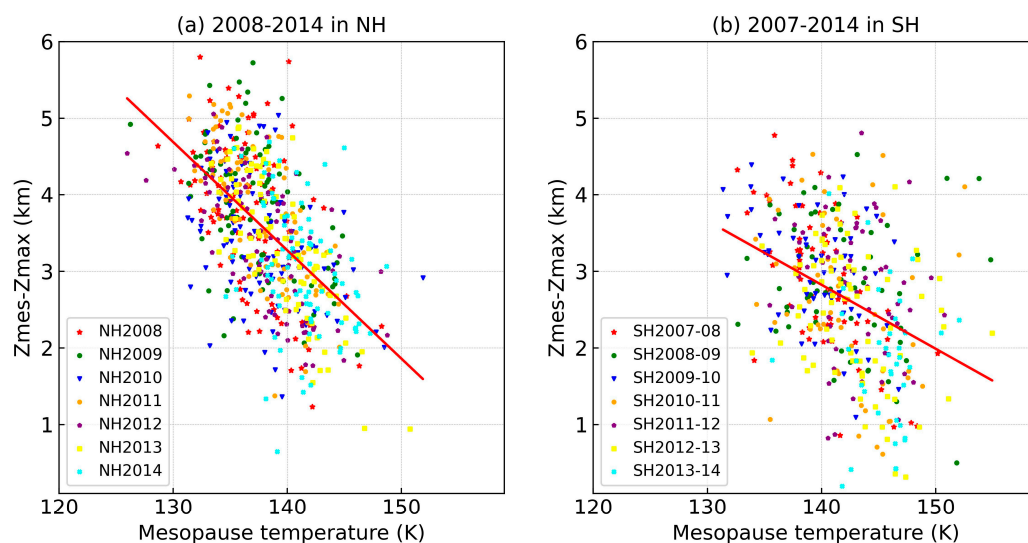
Figure 4. The correlation between Z_{mes}-Z_{max} and mesopause temperature using SOFIE observation data; (**a**) represents the NH seasons, (**b**) represents the SH seasons; the red lines represent the linear fitting results.

4. Analysis of Model Results

4.1. Typical Case Analysis under Different Mesopause Temperatures

From the results summarized in Section 2, it is evident that the mesopause temperature has a significant impact on Z_{mes}-Z_{max}. However, the factors influencing PMC height are not solely limited to temperature. Dynamic processes, such as planetary, tidal, and gravity waves, also play important roles in shaping the characteristics of PMCs, including their height and ice water content (IWC). In particular, gravity waves can affect the properties of PMCs by causing spatial and temporal disturbances in local temperature and water vapor. For example, in mid-latitude regions, where background atmospheric saturation is insufficient for cloud formation, a rapid temperature drop induced by gravity waves can lead to the occasional appearance of PMCs [2]. Alternatively, the fragmentation and dissipation of energy caused by gravity waves can heat the local atmosphere, resulting in a decrease in the

IWC and brightness of preexisting PMCs or even their complete dissipation [28]. Moreover, the influence of these dynamic processes becomes more pronounced when the background atmospheric temperature is high and approaches the critical threshold for cloud formation, known as the frost point temperature. This also partly explains the weaker correlation between the PMCs seasons in the SH, as shown in Figure 4b. In Section 3, the challenge of separating the effects of dynamic processes using available observational data is discussed. Therefore, the values of Z_{mes}-Z_{max} and its rate of change influenced by temperature do not represent the precise values under ideal conditions.

To further examine the correlation without excessive consideration of dynamic processes, this section utilizes a 0-D model of the PMCs. This model neglects the time dependence of microphysical processes, and its simulation results closely approximate the critical state of complex microphysical models [17]. By utilizing the background atmospheric temperature, water vapor, and pressure profiles observed by SOFIE as inputs, the 0-D model can calculate the cloud ice mass density profile. This information can be further used to compute important physical quantities such as cloud top, cloud bottom, peak height, and IWC. Subsequently, the simulated values of Z_{mes}-Z_{max} were compared with the observed mesopause temperatures from the SOFIE data to assess their correlation.

Figure 5 presents three cases of different background conditions: T_{mes} < 130 K, 130 K < T_{mes} < 140 K, and T_{mes} >140 K. Case 1 in Figure 5a shows the observation data from the 860th orbit in the NH in 2011, where the mesopause temperature was the lowest among the three cases, as shown in Table 1, with a value of only 123.3 K at an altitude of 88.4 km. The green curve represents the frost point temperature profile calculated by the 0-D model based on the observed pressure and water vapor conditions at that time. Once the actual temperature began to fall below the frost point temperature near 90.2 km, ice crystals started to form, resulting in the cloud top being located at 90.0 km. It can be seen that the cloud top, in this case, was higher than the mesopause altitude. As the altitude decreased, the atmospheric temperature remained below the frost point temperature. At this altitude (around 83.2 km), where the atmosphere was extremely sparse (about 10^{-3} hPa), ice crystals primarily grew through condensation and aggregation processes. As the ice crystals continued to grow and increase in number, the peak height of the PMCs, which is the altitude where the cloud ice mass density reaches its maximum value of 53.2 ng/m^3, was reached. Z_{mes}-Z_{max} in this case was 5.2 km. As the altitude continued to decrease, the atmospheric temperature erose, and ice crystals begam to gradually melt and sublime. When the frost point temperature was exceeded at 81.6 km, PMCs also disappeared at this altitude. For the entire case, the column integral of cloud ice mass density, i.e., the IWC, reached 154.2 ng/m^2, which indicates a strong case of PMCs.
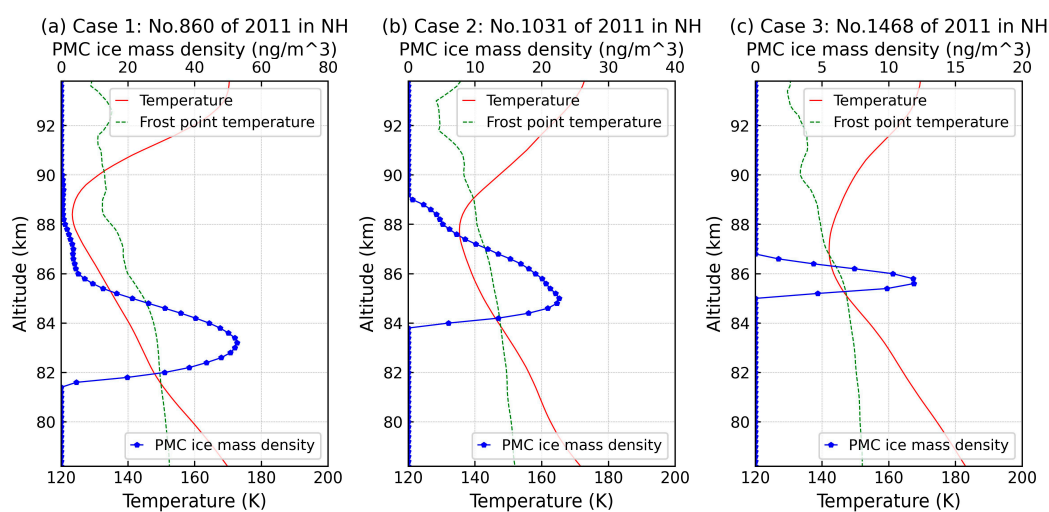
Figure 5. Three cases simulated based on the 0-D model under different background atmospheric conditions: (**a**) for Case 1, (**b**) for Case 2, (**c**) for Case 3.

Table 1. The parameters of three examples simulated based on the 0-D model.

Parameters	Case 1	Case 2	Case 3
Mesopause altitude/km	88.4	87.8	87.0
Peak height Z_{max}/km	83.2	85.0	85.6
Cloud top Z_{top}/km	90.0	89.0	86.6
Cloud bottom Z_{bot}/km	81.6	84.0	85.2
Ice water content IWC/(ng/m^2)	154.2	65.7	11.5
Mesopause temperature/K	123.3	135.3	142.1
Z_{mes}-Z_{max}/km	5.2	2.8	1.4

For Case 2, as shown in Figure 5b, the mesopause temperature was slightly higher at 135.3 K, and it descended to a height of 87.8 km. The atmospheric temperature dropped below the frost point temperature starting at 85.2 km and then reached its peak at a higher position of 85.0 km. Due to the limited number of temperature values below the frost point and the small vertical range of the cold region, the conditions and time for ice crystal condensation and growth were insufficient. Therefore, at the peak height, the cloud ice mass density was 22.8 ng/m^3, and the Z_{mes}-Z_{max} value was smaller than in Case 1, at 2.8 km. The IWC within the cloud was 65.7 ng/m^2, indicating a moderate-intensity individual case of PMCs. For Case 3, as shown in Figure 5c, the mesopause temperature was 142.1 K, and it descended to a height of 87.0 km. The atmospheric temperature only dropped below the frost point temperature between 85.2 km and 86.6 km, with the peak height of PMCs located at 85.6 km, higher than in the previous two cases. The Z_{mes}-Z_{max} value was only 1.4 km because of the short condensation growth distance. Consequently, the IWC within the cloud was only 11.5 ng/m^2, indicating a weaker individual case of PMCs.

4.2. Statistical Correlation for Years 2008–2014

In the same manner, as described in Section 2, we analyzed data from seven PMC seasons for the NH and SH from 2008 to 2014. The atmospheric temperature, water vapor, and pressure profiles were input into the 0-D model. The daily average simulated Z_{mes}-Z_{max} and mesopause temperatures from SOFIE are shown as scatter points in Figure 6. The blue line represents the linear regression modeling results, and the red line represents the linear regression results for the observed data from Figure 4, shown for comparison. As Figure 6a shows, for the seven seasons in the NH, we obtained valid data for 655 days. The correlation coefficient between Z_{mes}-Z_{max} and the mesopause temperature was −0.71. The linear regression relationship was given by the equation Z_{mes}-Z_{max} = −0.21T_{mes} + 31.79. The rate of change of Z_{mes}-Z_{max} with respect to the mesopause temperature was −0.21 km/K, which is greater than the observed value of −0.14 km/K. The average value of Z_{mes}-Z_{max} was 2.33 km. As Figure 6b shows, for the seven seasons in the SH, there were 515 days of valid data. The correlation coefficient was −0.62. The linear regression relationship was Z_{mes}-Z_{max} = −0.14T_{mes} + 21.15, with a rate of change of −0.14 km/K, which is greater than the actual observed value of −0.08 km/K. The average value of Z_{mes}-Z_{max} was 1.42 km. Compared with the observed data, the simulation results indicate a smaller Z_{mes}-Z_{max}, which is more easily influenced by the mesopause temperature.

Taking the results shown in Figures 5 and 6 together with an understanding of the mechanism of PMC formation, it can be concluded that the mesopause temperature determines the conditions for the formation and evolution of ice crystals within the cloud. Under conditions of relatively stable water vapor content in the mesopause region, lower atmospheric temperatures in that region resulted in a greater distance and longer time for ice crystal condensation and growth. With the assistance of natural gravity, this led to a lower sinking height, causing the peak height within the cloud to be further away from the mesopause.

Furthermore, although the input values for the 0-D model were based on observed data, the SOFIE limb observation mode had a horizontal field of view of approximately 200 km and an integrated path length in the line-of-sight direction of approximately 180 km.

This mode is not sensitive to small-scale disturbances (such as small-scale gravity waves). Therefore, by comparing the analysis results summarized in Sections 3 and 4, we can infer that disturbances in small-scale dynamic processes tend to enhance the background conditions for ice crystal growth within the clouds and weaken the influence of the mesopause temperature on the peak height of PMCs.
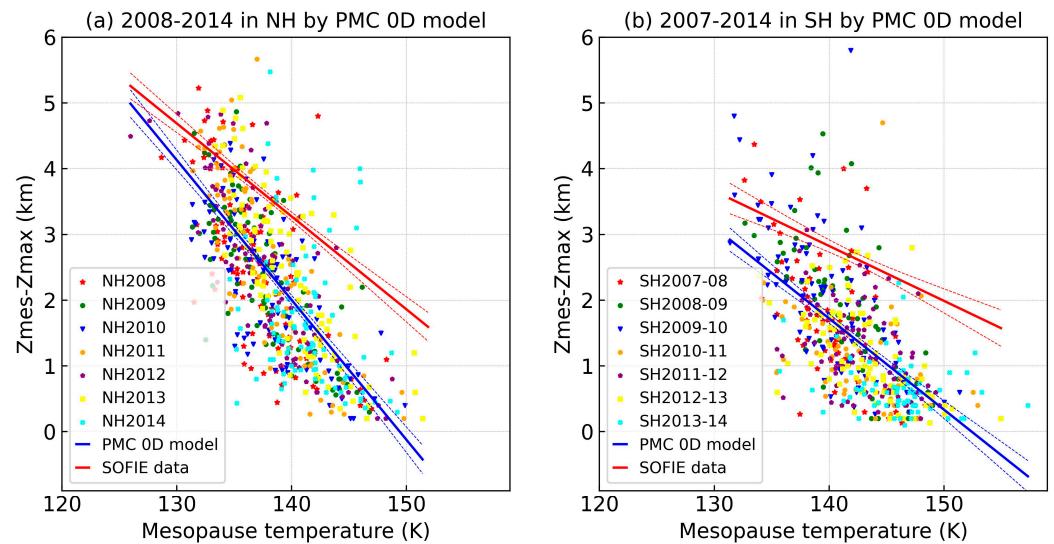
Figure 6. The correlation between Z_{mes}-Z_{max} using the PMC 0-D model and mesopause temperature observed by SOFIE; (**a**) represents the NH seasons, (**b**) represents the SH seasons; The blue lines represent the linear fitting results, while the red lines are the same as Figure 4; the dashed curves represent the confidence limits of 95%.

5. Conclusions

In this study, we used satellite observation data from SOFIE and a 0-D model to conduct a detailed investigation of the correlation between Z_{mes}-Z_{max} and atmospheric mesopause temperature. The main conclusions are as follows.

(1) Statistical analyses were conducted using satellite observation data from SOFIE for the seven PMC seasons from 2007 to 2014 in both the NH and SH. There was a clear negative correlation between the difference in height between the mesopause and the peak height of the PMCs (Z_{mes}-Z_{max}) and the atmospheric mesopause temperature. This correlation was smaller at the beginning and ending stages of the PMC seasons but larger in the middle of the seasons. For the NH, the correlation coefficient was -0.59, with an average Z_{mes}-Z_{max} value of 3.54 km and a rate of change of Z_{mes}-Z_{max} with respect to the mesopause temperature of -0.14 km/K. For the SH, the correlation coefficient was -0.37, with an average Z_{mes}-Z_{max} value of 2.66 km and a rate of change of Z_{mes}-Z_{max} with respect to the mesopause temperature of -0.08 km/K.

(2) An analysis of three typical cases simulated by the 0-D model also revealed significant negative correlations for the NH and SH, with greater correlation coefficients of -0.71 and -0.62, respectively. The average values of Z_{mes}-Z_{max} were 2.33 km and 1.42 km, and the rates of change of Z_{mes}-Z_{max} regarding the mesopause temperature were -0.21 km/K and -0.14 km/K for the NH and SH, respectively.

(3) Combining the condensation and sublimation mechanisms of PMC formation, it can be inferred that when the mesopause temperature is lower, the distance and time for ice crystal condensation and growth within the cloud will be greater, and the descent height will be lower. As a result, the peak height of the PMCs is further away from mesopause. In addition, disturbances in small-scale dynamic processes tend to weaken the influence of mesopause temperature on the peak height of the PMCs.

Institutional Review Board Statement: Not applicable.

Informed Consent Statement: Not applicable.

Data Availability Statement: The SOFIE PMC data are now available to the public in the form of summary files containing data for each PMC season at https://sofie.gats-inc.com/getdata_pmc (accessed on 5 August 2024).

Conflicts of Interest: The authors declare no conflicts of interest.

References

1. Dalin, P.; Perminov, V.; Pertsev, N.; Romejko, V. Updated long-term trends in mesopause temperature, airglow emissions, and noctilucent clouds. *J. Geophys. Res. Atmos.* **2020**, *125*, e2019JD030814. [CrossRef]
2. Miao, J.X.; Gao, H.Y.; Kou, L.L.; Zhang, Y.H.; Li, Y.; Chu, Z.G.; Bu, L.B.; Wang, Z. A case study of midlatitude noctilucent clouds and its relationship to the secondary-generation gravity waves over tropopause inversion layer. *J. Geophys. Res. Atmos.* **2022**, *127*, e2022JD036912. [CrossRef]
3. Thomas, G.E.; Olivero, J.J.; Jensen, E.J.; Schroeder, W.; Toon, O.B. Relation between increasing methane and the presence of ice clouds at the mesopause. *Nature* **1989**, *338*, 490–492. [CrossRef]
4. Hervig, M.; Thompson, R.E.; McHugh, M.; Gordley, L.L.; Russell, J.M., III; Summers, M.E. First confirmation that water ice is the primary component of polar mesospheric clouds. *Geophys. Res. Lett.* **2001**, *28*, 971–974. [CrossRef]
5. Hervig, M.E.; Berger, U.; Siskind, D.E. Decadal variability in PMCs and implications for changing temperature and water vapor in the upper mesosphere. *J. Geophys. Res. Atmos.* **2016**, *121*, 2383–2392. [CrossRef]
6. Gardner, C.S.; Papen, G.C.; Chu, X.; Pan, W. First lidar observations of middle atmosphere temperatures, Fe densities, and polar mesospheric clouds over the north and south poles. *Geophys. Res. Lett.* **2001**, *28*, 1199–1202. [CrossRef]
7. Petelina, S.V.; Llewellyn, E.J.; Degenstein, D.A.; Lloyd, N.D. Odin/OSIRIS limb observations of polar mesospheric clouds in 2001-2003. *J. Atmos. Sol. Terr. Phys.* **2006**, *68*, 42–55. [CrossRef]
8. Duft, D.; Nachbar, M.; Leisner, T. Unravelling the microphysics of polar mesospheric cloud formation. *Atmos. Chem. Phys.* **2019**, *19*, 2871–2879. [CrossRef]
9. Kaifler, N.; Baumgarten, G.; Klekociuk, A.R.; Alexander, S.P.; Fiedler, J.; Lübken, F.-J. Small scale structures of NLC observed by lidar at 69N/69S and their possible relation to gravity waves. *J. Atmos. Sol. Terr. Phys.* **2006**, *104*, 244–252. [CrossRef]
10. Thomas, G.E. Mesospheric clouds and the physics of the mesopause region. *Rev. Geophys.* **1991**, *29*, 553–575. [CrossRef]
11. Russell, J.M., III; Rong, P.; Bailey, S.M.; Hervig, M.E.; Petelina, S.V. Relationship between the summer mesopause and polar mesospheric cloud heights. *J. Geophys. Res.* **2010**, *15*, D16209. [CrossRef]
12. Sheese, P.E.; Llewellyn, E.J.; Gattinger, R.L.; Bourassa, A.E.; Degenstein, D.A.; Lloyd, N.D.; McDade, I.C. Mesopause temperatures during the polar mesospheric cloud season. *Geophys. Res. Lett.* **2011**, *38*, L11803. [CrossRef]
13. Siskind, D.E.; Merkel, A.W.; Marsh, D.R.; Randall, C.E.; Hervig, M.E.; Mlynczak, G.; Russell, J.M., III. Understanding the effects of polar mesospheric clouds on the environment of the upper mesosphere and lower thermosphere. *J. Geophys. Res. Atmos.* **2018**, *123*, 11705–11719. [CrossRef]
14. Bailey, S.M.; Merkel, A.W.; Thomas, G.E.; Carstens, J.N. Observations of polar mesospheric clouds by the Student Nitric Oxide Explorer. *J. Geophys. Res.* **2005**, *110*, D13203. [CrossRef]
15. Chu, X.; Nott, G.J.; Espy, P.J.; Gardner, C.S.; Diettrich, J.C.; Clilverd, M.A.; Jarvis, M.J. Lidar observations of polar mesospheric clouds at Rothera, Antarctica (67.5°S, 68.0°W). *Geophys. Res. Lett.* **2004**, *31*, L02114. [CrossRef]
16. Jensen, E.; Thomas, G.E. A growth-sedimentation model of polar mesospheric clouds: Comparison with SME measurements. *J. Geophys. Res.* **1988**, *93*, 2461–2473. [CrossRef]
17. Rapp, M.; Thomas, G.E. Modeling the microphysics of mesospheric ice particles: Assessment of current capabilities and basic sensitivities. *J. Atmos. Sol. Terr. Phys.* **2006**, *68*, 715–744. [CrossRef]
18. Lübken, F.-J.; Rapp, M.; Strelnikova, I. The sensitivity of mesospheric ice layers to atmospheric background temperatures and water vapor. *Adv. Space Res.* **2007**, *40*, 794–801. [CrossRef]
19. Rong, P.P.; Russell, J.M., III; Hervig, M.E.; Bailey, S.M. The roles of temperature and water vapor at different stages of the polar mesospheric cloud season. *J. Geophys. Res.* **2009**, *117*, D04208. [CrossRef]

20. Russell, J.M.; Bailey, S.M.; Gordley, L.L.; Rusch, D.W.; Horányi, M.; Hervig, M.E.; Thomas, G.E.; Randall, C.E.; Siskind, D.E.; Stevens, M.H.; et al. The Aeronomy of Ice in the Mesosphere (AIM) mission: Overview and early science results. *J. Atmos. Sol. Terr. Phys.* **2009**, *71*, 289–299. [CrossRef]
21. Hervig, M.E.; Stevens, M.H.; Gordley, L.L.; Deaver, L.E.; Russell, J.M., III; Bailey, S.M. Relationships between polar mesospheric clouds, temperature, and water vapor from Solar Occultation for Ice Experiment (SOFIE) observations. *J. Geophys. Res.* **2009**, *114*, D20203. [CrossRef]
22. Mauersberger, K.; Krankowsky, D. Vapor pressure above ice at temperatures below 170K. *Geophys. Res. Lett.* **2003**, *30*, 1121–1123. [CrossRef]
23. Murphy, D.M.; Koop, T. Review of the vapour pressures of ice and supercooled water for atmospheric applications. *Q. J. R. Meteorol. Soc.* **2005**, *131*, 1539–1565. [CrossRef]
24. Hervig, M.E.; Gordley, L.L.; Stevens, M.H.; Russell, J.M., III; Bailey, S.M.; Baumgarten, G. Interpretation of SOFIE PMC measurements: Cloud identification and derivation of mass density, particle shape, and particle size. *J. Atmos. Sol. Terr. Phys.* **2009**, *71*, 316–330. [CrossRef]
25. Wehr, T.; Kubota, T.; Tzeremes, G.; Wallace, K.; Nakatsuka, H.; Ohno, Y.; Koopman, R.; Rusli, S.; Kikuchi, M.; Eisinger, M.; et al. The EarthCARE mission–science and system overview. *Atmos. Meas. Tech.* **2023**, *16*, 3581–3608. [CrossRef]
26. Ren, K.; Gao, H.Y.; Niu, S.Q.; Kou, L.L.; Zhang, L.G.; Xie, Y.Q.; Bu, L.B. Simulation of polar mesospheric cloud measurements via spaceborne LiDAR and detection efficiency analysis. *Appl. Opt.* **2024**, *63*, 7056–7070. [CrossRef]
27. Gao, H.Y.; Shepherd, G.G.; Tang, Y.; Bu, L.B.; Wang, Z. Double-layer structure in polar mesospheric clouds observed from SOFIE/AIM. *Ann. Geophys.* **2017**, *35*, 295–309. [CrossRef]
28. Gao, H.Y.; Li, L.C.; Bu, L.B.; Zhang, Q.L.; Tang, Y.H.; Wang, Z. Effect of Small-Scale Gravity Waves on Polar Mesospheric Clouds Observed From CIPS/AIM. *J. Geophys. Res. Space Phys.* **2018**, *123*, 4026–4045. [CrossRef]